

# Localized Surface Plasmon-Enhanced Deep-UV Light-Emitting Diodes with Al/Al<sub>2</sub>O<sub>3</sub> Asymmetrical Nanoparticles

Jin Wang<sup>1</sup> · Guofeng Yang<sup>1,2</sup> · Qing Zhang<sup>1</sup> · Shumei Gao<sup>1</sup> · Rong Zhang<sup>2</sup> · Youdou Zheng<sup>2</sup>

Received: 26 March 2016 / Accepted: 6 July 2016 / Published online: 15 July 2016  
© Springer Science+Business Media New York 2016

**Abstract** In this work, light-extraction enhancement induced by localized surface plasmons (LSPs) on asymmetrical design of metallic nanoparticles (NPs) for AlGaN deep-ultraviolet (UV) light-emitting diodes (LEDs) is investigated numerically. The systems under study consist of Al NPs with varying diameter separated by a nano-gap, and the symmetrical dimer NPs with different geometrical parameters are studied for reference. We have demonstrated that tunable plasmonic NPs and spectral response can be controlled by varying the size of the nanoparticles and nano-gaps. It is found that the enhancement of the electric field and the peak position are subject to geometrical characteristics of the NP components in different manners for symmetrical and asymmetrical systems, respectively. High enhancement ratio for UV wavelength can be obtained by tuning parameters of asymmetrical system, which is potential for improving the performance of deep-UV LEDs.

**Keywords** Localized surface plasmon resonance · Deep-ultraviolet light-emitting diodes · Light-extraction efficiency · Finite difference time domain method

## Introduction

The AlGaN-based deep-ultraviolet light-emitting diodes (deep-UV LEDs, radiation with a wavelength ranging from 200 to 350 nm) have given much attention for their various applications, such as fluorescence-based sensing, high density optical data storage, and biological detection [1–3]. It has reported that deep-UV LEDs at a wavelength of 280 nm with the upper limit of internal quantum efficiency (IQE) as high as 70 % [4]. However, one bottleneck in the adoption of deep-UV LED is the relatively low efficiency of these devices, which is limited by low light-extraction efficiency (LEE) caused by total internal reflection and dominant TM-polarized spontaneous emission [5, 6].

It is well known that some nanoparticles (NPs) could lead to a localized surface plasmon resonance (LSPR) phenomenon, an effect that produces collective oscillations of a nanoparticle's conduction band electrons, resulting in strong peaks in extinction spectra, as well as strong enhancement of the local electromagnetic fields surrounding the NPs [7, 8]. In other words, the radiating dipole transfers energy into the surface plasmon (SP) for emission, analogous to amplified spontaneous emission. SP coupling is particularly useful for increasing emission efficiency of a light-emitting device of inherent low IQE. In addition, it is noted that SP can also have influence on LEE besides the aforementioned effective IQE increase in a device [9].

Recent advances in fabrication technologies have made it possible to synthesize all kind of particles with different sizes and geometries, which exhibit wide range of potential applications such as highly sensitive optical nanosensors, biochemistry, and solar cells [10–12]. Previous researches have demonstrated that the LSPR is sensitively and intimately related to particles' sizes, geometries, interparticle spacings, compositions, and location environments [13–15]. There are a lot of studies that have reported the LSPR resonance position could

---

✉ Guofeng Yang  
gfyang@jiangnan.edu.cn

✉ Shumei Gao  
gaosm@126.com

<sup>1</sup> School of Science, Jiangsu Provincial Research Center of Light Industrial Optoelectronic Engineering and Technology, Jiangnan University, Wuxi 214122, China

<sup>2</sup> School of Electronic Science and Engineering, Nanjing University, Nanjing 210093, China

be regulated at a wide spectroscopic range by only changing the sizes of the metallic NPs [16]. Taguchi et al. reported that the LSPR peaks were changed from 340 to 270 nm only by varying the size of Al nanostructures from 80 to 50 nm in UV-LED [17], and Henson et al. demonstrated that the measured PL enhancement factors are strongly dependent on the NP array dimensions [18].

In this work, we numerically investigate the enhanced LEE performance through the energy transfer between quantum wells (QWs) and localized surface plasmons (LSPs) induced by nanoparticle embedded in deep-UV LEDs based on AlGaIn materials. To the best of our knowledge, relevant work previously published mainly focused on nano-metallic structures with uniform geometry, such as large uniform arrays or films. Different from previous studies, our work features breaking uniformity of the system and including tuning of asymmetrical structures besides symmetrical ones, in order to demonstrate asymmetrical nanostructures would be potential for improving the deep-UV LEDs' performance.

## Structures and Simulation

It is well known that uncoupled SPs resonance energy of Aluminum (Al) approaches the photon energy emitted by AlGaIn-based deep-UV LED, so the Al NPs are employed in this work. Unlike noble metals, Al is easily oxidized when exposed to the atmosphere; therefore, Al/Al<sub>2</sub>O<sub>3</sub> core-shell based nano-components were designed in our calculation [19], the thickness of the Al<sub>2</sub>O<sub>3</sub> shell is about 3 nm for the simulation according to previous report [20]. The nano-Al/Al<sub>2</sub>O<sub>3</sub> core-shell structure system under investigation is composed of a pair of Al/Al<sub>2</sub>O<sub>3</sub> components (particle shapes) deposited on the surface of p-GaN layer. The active region (QWs and barrier) of a typical DUV-AlGaIn LED is a few nanometers thick, and by varying the Al composition in the AlGaIn quantum wells and barriers, its emission peak can slightly shift around 300 nm. In this numeric investigation, for calculating the extinction spectra, the incident wave was excited by a plane wave source at a given position under the NPs to propagate from the infinite half-space substrate in the total-field scattered-field. A dipole source has been used to simulate the photon generation process inside AlGaIn multiple quantum wells (MQWs) for the calculation of LEE. Both source wavelengths were set with a bandwidth around 200 nm and centering at 300 nm, which is wide enough to cover the entire linewidth in general deep-UV LEDs [21, 22].

The SP fringing field penetration depth into GaN medium is given by

$$L = \frac{\lambda}{2\pi} \left( \frac{\varepsilon_{\text{GaN}}^R + \varepsilon_{\text{Al}}^R}{\varepsilon_{\text{GaN}}^2} \right)^{\frac{1}{2}} \quad (1)$$

Where  $\varepsilon_{\text{GaN}}^R$  and  $\varepsilon_{\text{Al}}^R$  are the real part of the dielectric constants of the GaN and Al, respectively. In this study, the GaN medium is set with dielectric constant of 6.25. The penetration depth  $L$  was estimated to be 33.5 nm for QW-SP coupling at the wavelength of 300 nm for a UV-LED.

The LEE for a LED is defined as the fraction of the optical power generated in the active layer of the LED that escapes into the air above the LED within a desired range of angles, which can be calculated by

$$LEE = \frac{\gamma_{\text{rad}}}{\gamma_{\text{rad}} + \gamma_{\text{loss}}} \quad (2)$$

where  $\gamma_{\text{rad}}$  denotes the decay rate of the excitations to photons that can be extracted from the LED device;  $\gamma_{\text{loss}}$  is the photons that can be lost in the LED device including photons absorbed in lossy material, trapped by total internal reflection (TIR) in high index layers and so on.

The schematic cross section of the system is shown in Fig. 1. The closely packed two nano-Al/Al<sub>2</sub>O<sub>3</sub> particles lie on the p-GaN with diameters  $d_1$  and  $d_2$  are separated by a gap  $D$ . The 20-nm-thick p-AlGaIn electron blocking layer (EBL) is positioned below the 10-nm-thick p-GaN layer to enable LSP coupling. Then followed by five AlGaIn MQWs, the thickness of QWs is set at 8 nm, and refractive indices of AlGaIn and GaN are 2.1 and 2.4, respectively. The dipole polarized parallel to the surface (TE-polarized dipole) is set at the midpoint of their geometrical center connecting line, which is the position in the center of AlGaIn QWs. The spatial nonuniform-grid finite difference time domain (FDTD) method is worked for saving the computational memory. For accurate representation of rapidly changing SP field, the maximum grid size is fixed as 1 nm, which is an adequate size to resolve the strongly localized field distribution in view of limited computational capacity. For accurate exquisite field distribution, the grid size in medium and sub-cells with finer size are deployed at certain positions as necessary. To simulate the infinite extension of the background environment, the entire region is placed by perfectly matched layer (PML) conditions on all the sides, and the whole system is merged into air with dielectric constant. Monitors are set up for the storage of

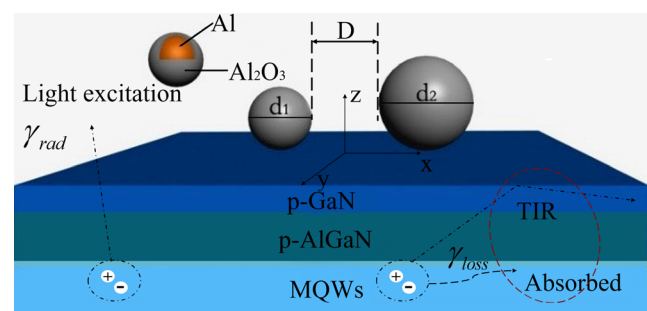


**Fig. 1** Schematic diagram of the asymmetrical structure for simulation

EM field data during iteration as well as the total radiation power is obtained by integrating the power flux through the monitor box surrounding the dipole source. And the extracted power is calculated by integrating the power flux through the monitor plane above the p-GaN surface.

### Results and Discussion

The simulated extinction spectra of a single Al/Al<sub>2</sub>O<sub>3</sub> NP are shown in Fig. 2. All spectral peak positions of the plasmonic resonance occur in the UV region with the diameters of Al/Al<sub>2</sub>O<sub>3</sub> NPs vary from 10 to 100 nm. Each curve has two or more peaks. Moreover, the Al NP size plays an important role on the spectral peak positions of the LSPR, the highest peak position shifts from 184 to 214 nm as the diameter of Al/Al<sub>2</sub>O<sub>3</sub> NP increases from 30 to 100 nm. This would be explained by that the sized NPs vary in the SP absorption wavelength contributes to overlapped with different frequency. Moreover, the resonance amplitude enhances with increasing the diameter of Al/Al<sub>2</sub>O<sub>3</sub> NP. It has reported that larger Al NPs could excite more electromagnetic energy due to their large absorption cross sections, higher polarizabilities, and larger radiative rates [23], thus resulting in higher resonance intensities.

Figure 3 shows the LEE enhancement ratio as a function of wavelength for two identical nano-Al/Al<sub>2</sub>O<sub>3</sub> particles closely separated by a fixed gap  $D = 10$  nm. All the enhancement peaks are controlled in the bandwidth of typical deep UV-LED, and the LEE of a deep UV-LED is generally enhanced when Al/Al<sub>2</sub>O<sub>3</sub> particles are used. The highest enhancement is obtained at  $d_1 = d_2 = 90$  nm with a peak position at about 264 nm. It can be found that the enhancement peaks on the curves red shift from 220 to 276 nm as the diameter of Al/

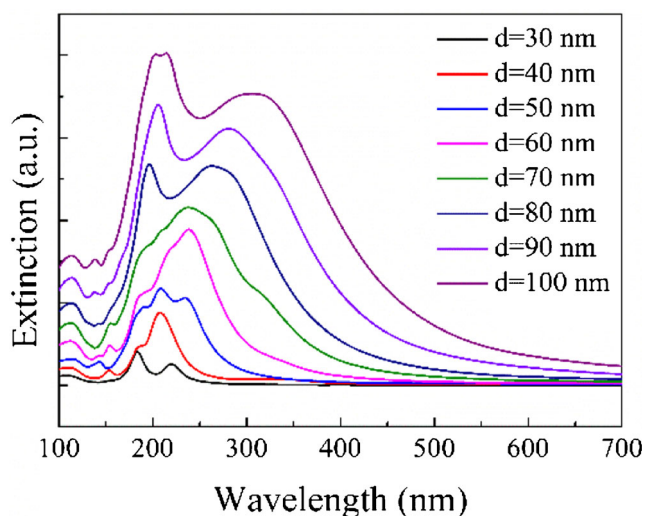


**Fig. 2** Normalized extinction spectra of a single Al/Al<sub>2</sub>O<sub>3</sub> core-shell nano-sphere

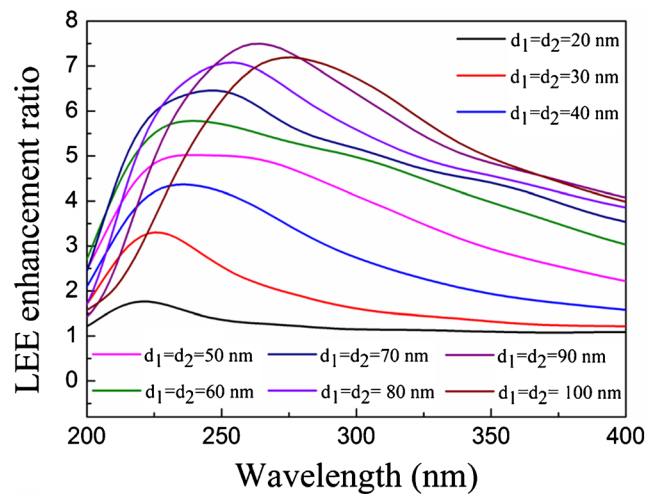
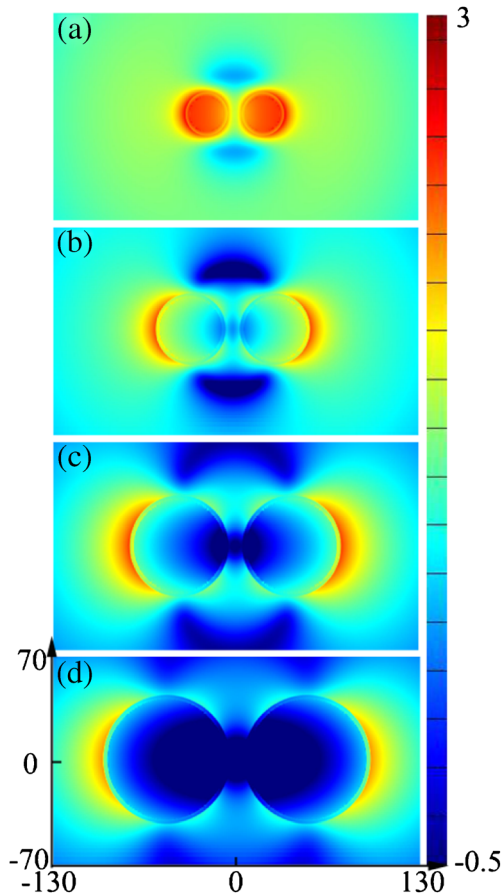


**Fig. 3** Enhancement ratio of LEE as a function of wavelength for two identical nano-Al/Al<sub>2</sub>O<sub>3</sub> particles separated by a fixed gap  $D = 10$  nm

Al<sub>2</sub>O<sub>3</sub> particles increase from 20 to 100 nm, correspondingly, and the magnitude of enhancement ratios are simultaneously increased. The enhancement of LEE would be relevant to the self-coupling of SPs on NPs, and further increased diameter of the NPs could result in stronger self-coupling of SPs, which renders invalidation of SP energy-momentum dispersion relation [24]. It is noted that the magnitude of enhancement ratio is declined for NPs diameter exceeding 90 nm, which is attributed to that larger metal particles dissipation can cause SP loss.

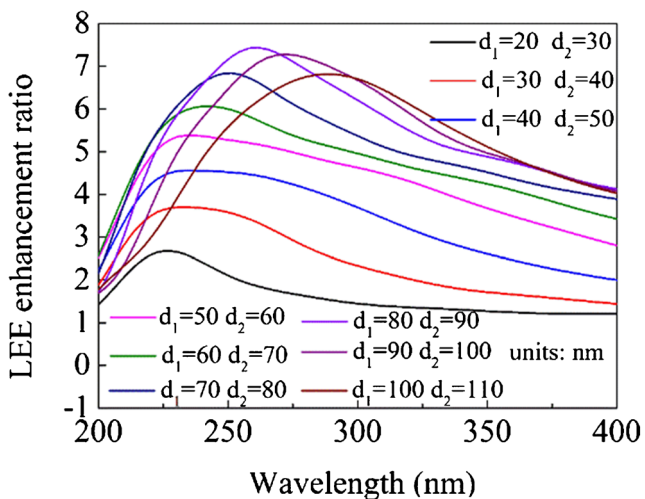
In order to verify the enhancement induced by SPs resonance, E-field intensity distribution ( $\log_{10}|E|^2$ , evaluated at the peak wavelengths) on the slice cutting through spherical centers in parallel with  $x$ - $y$  plane around two identical Al/Al<sub>2</sub>O<sub>3</sub> particles with diameter of (a) 30 nm, (b) 50 nm, (c) 70 nm, and (d) 90 nm are showed in Fig. 4, in all of which enhanced SP resonant field can be observed on the surfaces of nanoparticles. The distribution of E-field intensity around the particles has a radially symmetric shape and shows the highest value on the equator plane, which is an evidence for the SPs resonance when Al/Al<sub>2</sub>O<sub>3</sub> particles are used. The comparison of magnitude of the E-field intensity distribution can also be distinguished by the profiles that the identical NPs with a diameter of 90 nm (shown in Fig. 4d) reveal the highest peak intensity and largest area of high intensity region, which is in good agreement with the curves of LEE enhancement ratio in Fig. 3.

Figure 5 depicts the LEE enhancement ratio under an incident wave from 200 to 400 nm for asymmetrical dimer which contains two nano-Al/Al<sub>2</sub>O<sub>3</sub> particles closely separated by a fixed gap  $D = 10$  nm, various asymmetrical dimer with different diameters are designed to investigate the effect of the nanoparticle diameter on the LEE enhancement. It can be seen that the LEE enhancement ratio reaches the highest value at 261 nm, with an enhancement ratio of 7.43 at  $d_1 = 80$  nm  $d_2 = 90$  nm. The wavelength of the maximum enhancement ratio shows a 3-nm blue shift compared



**Fig. 4** E-field profiles ( $\log_{10}|E|^2$ ) distribution on the  $x$ - $y$  plane for simulation system with two identical Al/Al<sub>2</sub>O<sub>3</sub> particles with diameter of **a** 30 nm **b** 50 nm **c** 70 nm, and **d** 90 nm, respectively

with the symmetrical nano-Al/Al<sub>2</sub>O<sub>3</sub> particles with diameters fixed at  $d_1 = d_2 = 90$  nm. It also can be found that the maximum peak points on the curves show a red shift from 228 to 288 nm as the diameter of asymmetrical dimer increases from the  $d_1 = 20$  nm,  $d_2 = 30$  nm to  $d_1 = 100$  nm,  $d_2 = 110$  nm. Moreover, the peak



**Fig. 5** Enhancement ratio of LEE as a function of wavelength for asymmetrical nano-Al/Al<sub>2</sub>O<sub>3</sub> particles with different diameters

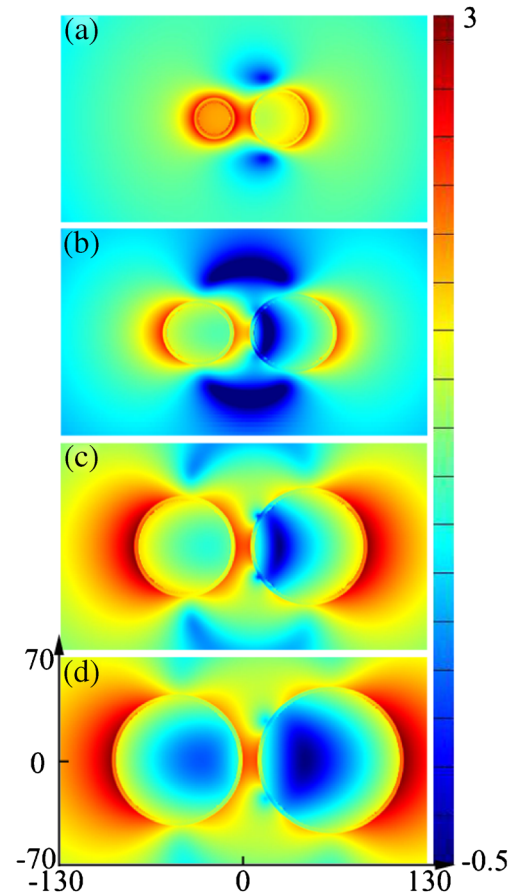


**Fig. 6** E-field profiles ( $\log_{10}|E|^2$ ) distribution on the  $x$ - $y$  plane for simulation system with two asymmetrical dimers **a**  $d_1 = 30$  nm,  $d_2 = 40$  nm; **b**  $d_1 = 50$  nm,  $d_2 = 60$  nm; **c**  $d_1 = 70$  nm,  $d_2 = 80$  nm; and **d**  $d_1 = 90$  nm,  $d_2 = 100$  nm, respectively

wavelength of the highest enhancement ratio is about 265 nm, with an enhancement ratio of 7.08 for the two particles with diameter of  $d_1 = 80$  nm and  $d_2 = 95$  nm (not shown here). As observed, the magnitude of enhancement ratio is generally

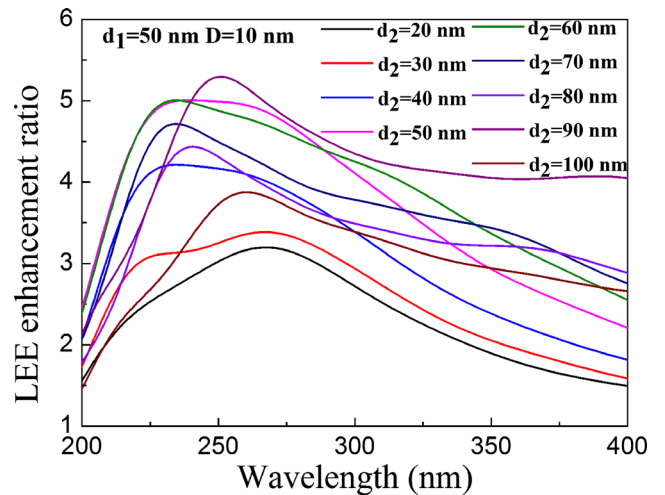


**Fig. 7** Enhancement ratio of LEE as a function of wavelength for asymmetrical dimer with fixed  $d_1 = 50$  nm and  $D = 10$  nm

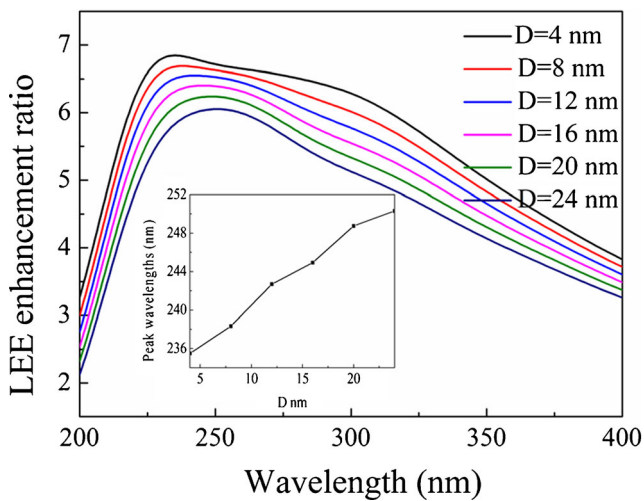


**Fig. 8** Enhancement ratio of LEE as a function of wavelength for asymmetrical nano-Al/Al<sub>2</sub>O<sub>3</sub> particles with different gaps

increased with the diameter of asymmetrical dimer, however, and further to improve the diameter thus reduce the peak position's enhancement ratio, which showed a similar trend with the symmetry system. The E-field distribution has been simulated to explain the enhanced performance of the asymmetrical dimer structures. Figure 6 shows the E-field intensity distribution ( $\log_{10}|E|^2$ , evaluated at the peak wavelengths) on the slice cutting through spherical centers in parallel with *x-y* plane around two asymmetrical dimer with diameter of (a)  $d_1 = 30$  nm,  $d_2 = 40$  nm; (b)  $d_1 = 50$  nm,  $d_2 = 60$  nm; (c)  $d_1 = 70$  nm,  $d_2 = 80$  nm; and (d)  $d_1 = 90$  nm,  $d_2 = 100$  nm, in all of which enhanced SP resonant field can be observed by the same phenomenon as aforementioned. Enhanced SPs resonant field can also be seen on the surfaces of the NPs, and the intensities are at the same level. However, it is evident that the profiles feature asymmetrical field distribution, in which higher intensity region is constrained on the surface of nanoparticle with larger diameter in each pair.

Asymmetrical dimer systems are also investigated by tweaking diameter of one NP varying from 20 to 100 nm whereas keeping the other one constant at 50 nm. As mentioned before, the wavelength of the highest LEE enhancement ratio with asymmetrical dimer structure ( $d_1 = 80$  nm,  $d_2 = 90$  nm) showed 3-nm blue shift compared with two identical nano-Al/Al<sub>2</sub>O<sub>3</sub> particles which diameters are fixed at  $d_1 = d_2 = 90$  nm. Motivated by the desire to comprehend the phenomena, we calculated the peak wavelength

of the highest LEE enhancement ratio when the diameters of the one nanoparticle are kept fixed to  $d_1 = 50$  nm and the other are varied from 20 to 100 nm. In Fig. 7, we illustrate the variation of the LEE enhancement ratio against the nanoparticle structures which the gaps are fixed at  $D = 10$  nm. It can be seen that the LEE enhancement ratio is always larger than 150 % in the spectral range of 200–400 nm. Even though the LEE is enhanced in those spectral ranges, the peak wavelengths of the highest LEE enhancement ratio are different. When the size of one nanoparticle is fixed at 50 nm, the wavelength of the maximum enhancement ratio shows blue shift with the diameter of the other nanoparticle increases to 40 nm. Further increasing the diameter of the other nanoparticle to 100 nm, the peak wavelength of the highest LEE enhancement ratio then shows a red shift. The highest magnitude of enhancement ratio is generally lower than that in Figs. 3 and 5, which could be explained by the Mie scattering.

In order to investigate the influence of the gaps on the LEE enhancement ratio. Two nano-Al/Al<sub>2</sub>O<sub>3</sub> particles with different size separated by a gap distance from 4 to 24 nm were designed, and the diameters of the two particles are fixed at 50 and 60 nm, respectively. In Fig. 8, we illustrate the enhancement ratio of LEE as a function of wavelength for asymmetrical nano-Al/Al<sub>2</sub>O<sub>3</sub> particles with different gaps. It is clear that the intensity increases monotonically with the decrease of the inter-sphere gap. The inset plots the peak wavelength of the LEE enhancement ratio as a function of the gap, and the peak wavelength of the LEE enhancement ratio varies linearly with the gap. In view of these observations, we can conclude that the asymmetrical metallic dimer structure has excellent spectral tenability by varying the diameters and gap distance of the nanoparticles. This opens up a number of opportunities for applications where sensitive spectral response against the system parameters for deep-UV LEDs.

### Conclusion

In conclusion, SP resonance-enhanced LEE induced by nano-Al/Al<sub>2</sub>O<sub>3</sub> particles based on deep-UV light-emitting diodes is numerically investigated. The enhancement is achieved by nano-Al/Al<sub>2</sub>O<sub>3</sub> particles systems consist of two symmetrical and asymmetrical dimers. The peak position and the

**Table 1** LEE enhancement information for Al/Al<sub>2</sub>O<sub>3</sub> NPs

Structures	Symmetrical dimer	Asymmetrical dimer	
Under research geometries (nm)	$d_1 = d_2 = 20 \sim 100$	$d_1 = 20 \sim 100, d_2 = d_1 + 10$	$d_1 = 50, d_2 = 20 \sim 100$
Highest enhancement ratio/wavelength (nm)	$7.50/\lambda = 264$	$7.43/\lambda = 216$	$5.29/\lambda = 251$
Highest enhancement geometry (nm)	$d_1 = d_2 = 90$	$d_1 = 80, d_2 = 90$	$d_1 = 50, d_2 = 90$
Peak position range (nm)	220 ~ 276	228 ~ 288	234 ~ 267

$D = 10$  nm, the thickness of Al<sub>2</sub>O<sub>3</sub> is 3 nm, LEE enhancement and peak position depends strongly on the size of the NPs

enhancement magnitude level of symmetrical as well as asymmetrical systems are compared, as shown in Table 1. It can be found that the enhancement level as well as peak position of the strong enhancement are subject to the change of geometry of NPs. For the symmetrical systems, increasing the diameter of two identical nano-Al/Al<sub>2</sub>O<sub>3</sub> particles can lead to the increase of enhancement magnitude and shifting of peak position; however, the magnitude of enhancement ratio is declined for NP diameter exceeding 90 nm. As for asymmetrical systems, by changing the radius of one of the NPs, a distinct shift is observed. The peak position shows blue shift firstly when the diameter of one NP increases to same as another NP and then shows red shift when the diameter is further increased. It is also shown that LEE enhancement and peak position depends strongly on the size of the nano-gap. It is believed that the fabrication of size-tunable Al NP arrays can potentially be applied to the design of practical LSP-enhanced AlGaIn-based deep UV-LEDs with high LEE.

**Acknowledgments** This work is supported by the China Postdoctoral Science Foundation (Nos. 2014M561623, 2014M551559), National Natural Science Foundation of Special Theoretical Physics (No. 11547168), and Natural Science Foundation of Jiangsu Province (Nos. BK20150158, BM2014402), Jiangsu Planned Projects for Postdoctoral Research Funds (No. 1401013B), the Fundamental Research Funds for Central Universities (Nos. JUSRP51628B, JUSRP51517), Anhui Provincial Natural Science Foundation (No. 1508085MF135), and Undergraduate Training Programs for Innovation of Jiangnan University (No. 2015309Y).

## References

- Davitt K, Song YK, Patterson WR, Nurmikko AV, Gherasimova M, Han J, Chang RK (2005) 290 and 340 nm UV LED arrays for fluorescence detection from single airborne particles. *Opt Express* 13(23):9548–9555
- Orton JW, Foxon CT (1998) Group III nitride semiconductors for short wavelength light-emitting devices. *Rep Prog Phys* 61(1):1–4
- Alimova A, Katz A, Sriramoju V, Budansky Y, Bykov AA, Zeylikovich R, Alfano RR (2007) Hybrid phosphorescence and fluorescence native spectroscopy for breast cancer detection. *J Biomed Opt* 12(1):014004
- Shatalov M, Yang J, Sun W, Kennedy R, Gaska R, Liu K (2009) Efficiency of light emission in high aluminum content AlGaIn quantum wells. *J Appl Phys* 105(7):073103
- Huang K, Gao N, Wang C, Chen X, Li J, Li S (2014) Top- and bottom-emission-enhanced electroluminescence of deep-UV light-emitting diodes induced by localised surface plasmons. *Sci Rep* 4
- Gao N, Huang K, Li J, Li S, Yang X, Kang, J (2012) Surface-plasmon-enhanced deep-UV light emitting diodes based on AlGaIn multi-quantum wells. *Sci Rep* 2
- Okamoto K, Niki I, Shvartser A, Narukawa Y, Mukai T, Scherer A (2004) Surface-plasmon-enhanced light emitters based on InGaIn quantum wells. *Nat Mater* 3(9):601–605
- Okamoto K, Niki I, Scherer A, Narukawa Y, Mukai T, Kawakami Y (2005) Surface plasmon enhanced spontaneous emission rate of InGaIn/GaN quantum wells probed by time-resolved photoluminescence spectroscopy. *Appl Phys Lett* 87(7):071102
- Kuo Y, Ting SY, Liao CH, Huang JJ, Chen CY, Hsieh C, Yang CC (2011) Surface plasmon coupling with radiating dipole for enhancing the emission efficiency of a light-emitting diode. *Opt Express* 19(Suppl 4):A914–A929
- Vilela D, Gonzalez MC, Escarpa A (2012) Sensing colorimetric approaches based on gold and silver nanoparticles aggregation: chemical creativity behind the assay. *Anal Chim Acta* 751:24–43
- Zhang LL, Ma FF, Kuang YF, Cheng S, Long YF, Xiao QG (2016) Highly sensitive detection of bovine serum albumin based on the aggregation of triangular silver nanoplates. *Spectrochim Acta A Mol Biomol Spectrosc* 154:98–102
- Green MA, Pillai S (2012) Harnessing plasmonics for solar cells. *Nat Photonics* 6(3):130–132
- Sherry LJ, Chang SH, Schatz GC, Van Duyne RP, Wiley BJ, Xia Y (2005) Localized surface plasmon resonance spectroscopy of single silver nanocubes. *Nano Lett* 5(10):2034–2038
- Sherry LJ, Jin R, Mirkin CA, Schatz GC, Van Duyne RP (2006) Localized surface plasmon resonance spectroscopy of single silver triangular nanoprisms. *Nano Lett* 6(9):2060–2065
- Huang WY, Qian W, El-Sayed MA (2004) Coherent vibrational oscillation in gold prismatic monolayer periodic nanoparticle arrays. *Nano Lett* 4(9):1741–1747
- Bouali A, Haxha S, AbdelMalek F, Dridi M, Bouchriha H (2014) Tuning of plasmonic nanoparticle and surface enhanced wavelength shifting of a nanosystem sensing using 3-D-FDTD method. *IEEE J Quantum Electron* 50(8):651–657
- Taguchi A, Saito Y, Watanabe K, Yijian S, Kawata S (2012) Tailoring plasmon resonances in the deep-ultraviolet by size-tunable fabrication of aluminum nanostructures. *Appl Phys Lett* 101(8):081110
- Henson J, Dimakis E, DiMaria J, Li R, Minissale S, Dal Negro L, Paiella R (2010) Enhanced near-green light emission from InGaIn quantum wells by use of tunable plasmonic resonances in silver nanoparticle arrays. *Opt Express* 18(20):21322–21329
- Chan GH, Zhao J, Schatz GC, Van Duyne RP (2008) Localized surface plasmon resonance spectroscopy of triangular aluminum nanoparticles. *J Phys Chem C* 112(36):13958–13963
- Knight MW, King NS, Liu L, Everitt HO, Nordlander P, Halas NJ (2014) Aluminum for plasmonics. *ACS Nano* 8(1):834–840
- Shur MS, Gaska R (2010) Deep-ultraviolet light-emitting diodes. *IEEE Trans Electron Dev* 57(1):12–25
- Hirayama H, Fujikawa S, Kamata N (2015) Recent progress in AlGaIn-based deep-UV LEDs. *Electron Commun Jpn* 98(5):1–8
- Fan X, Zheng W, Singh DJ (2014) Light scattering and surface plasmons on small spherical particles. *Light-Sci Appl* 3:e179
- Lin YZ, Liu DY, Gao JW (2015) Numeric tuning of surface plasmon enhanced spontaneous emission induced by Nano-metallic particle systems embedded in GaIn-based LED. *J Disp Technol* 11(3):296–303